npj | Climate and Atmospheric Science

www.nature.com/npjclimatsci

ARTICLE OPEN

Check for updates

New particle formation from agricultural recycling of organic waste products

R. Ciuraru[1]✉, J. Kammer[1], C. Decuq[1], M. Vojkovic[2], K. Haider[1,2], Y. Carpentier[2], F. Lafouge[1], C. Berger[1], M. Bourdat-Deschamps[1], I. K. Ortega[3], F. Levavasseur[1], S. Houot[1], B. Loubet[1], D. Petitprez[3] and C. Focsa[2]

Secondary organic aerosols (SOA) are one of the main sources of uncertainty in the current understanding of the Earth's climate. Agriculture contributes to primary aerosol emissions, but there is no estimate of SOA formation from gaseous precursors. Organic waste products such as sewage sludge are applied to cropland as fertilizers. In this work, we show that sewage sludge is an unaccounted source of nucleation precursors, such as skatole (C_9H_9N). Skatole emission and nucleation rates up to 1.1×10^6 cm^{-3} s^{-1} owing to ozone reactivity were measured in the laboratory. Our results show that SO_2 plays a key role in the oxidation of skatole and leads to intensive new particle formation. The products of ozone reactions with skatole and the possible ozonolysis reaction mechanism are discussed. This nucleation mechanism might aid our understanding of the organic waste agricultural recycling contribution to the aerosol balance in the atmosphere. Based on the measured particle emission flux, the surface area of sewage sludge spread in France and the time before sewage sludge incorporation into the soil, a rough estimate of the annual quantity of particles generated by this agricultural activity is in the range of one ton, which represents ~0.03% of the total $PM_{1.0}$ emissions from the agricultural and forestry sectors in France. As spreading occurs over only a few days (mid-summer), these emissions may locally be of great concern for local and regional air quality during this period of the year.

npj Climate and Atmospheric Science (2021)4:5 ; https://doi.org/10.1038/s41612-021-00160-3

INTRODUCTION

Atmospheric aerosols constitute a major human health concern and impact Earth's radiative balance both directly and indirectly through their influence on cloud properties. Atmospheric aerosols act as cloud condensation nuclei, thus altering cloud albedo, structure, and lifetime. They also represent a major health and economic issue, as particulate pollution is responsible for approximately three million premature deaths per year, which is projected to increase to six million by 2050[1]. Volatile organic compounds (VOCs), emitted into the atmosphere from anthropogenic and biogenic sources, are major players in atmospheric photochemical reactions that contribute to ozone formation. VOCs are also responsible for secondary organic aerosol (SOA) formation in the presence of photo-oxidants[2].

As revealed by different model simulations and laboratory studies, the most important source of atmospheric aerosols, in terms of the number concentration and proportion of climate-relevant particles, is new particle formation (NPF) and growth[3]. However, the nucleation mechanism leading to NPF remains poorly understood. Sulfuric acid has been identified as a key compound in atmospheric NPF[4]; however, its concentration in the atmosphere is too low to explain the observed nucleation rates, so additional compounds need to be identified[4]. Base compounds such as ammonia[5] or amines[6] have been proven to stabilize sulfuric acid clusters, leading to nucleation rates similar to those observed in the atmosphere. In addition, highly oxygenated molecules (HOMs) coming from the oxidation of VOCs can also stabilize sulfuric acid clusters[7], and a recent study[8] found that HOMs are able to form particles without the participation of sulfuric acid.

The formation of these compounds from ozonolysis of monoterpenes has been quantified[9], and modeling studies have quantified their formation in the atmosphere and their role in air quality[10,11]. However, our understanding of the processes involved in the formation and ageing of organic aerosols remains very limited but entirely necessary to improve the robustness of the models[12].

It is now well-known that agriculture and its activities affect local, regional, and global air quality, and global climate via not only significant ammonia (NH_3) and greenhouse gas (GHG) emissions but also VOC and aerosol emissions[13]. In some regions (e.g., eastern USA, Europe, Russia, and East Asia), agricultural emissions are estimated to be the largest relative contribution to $PM_{2.5}$[14]. Agriculture also represents a major ground-level ozone sink[15]. A wide variety of pollutants and GHGs, especially nitrogen-containing compounds, are emitted to the atmosphere from agricultural activities, including fertilizer use, farm machinery operation and livestock manure spreading. In particular, in France, agriculture is estimated to generate approximately one-third of the annual particle emissions (e.g., from livestock housing and tilling activities), but this estimate remains highly uncertain[16]. While great efforts have been made to estimate GHG and NH_3 emissions from agriculture and explore ways to abate them, knowledge about other pollutants, particularly SOA and VOC precursors, emitted by this sector is still scarce. Agricultural activities involving fertilizers or pesticides are also known to emit VOCs with high SOA formation potential[14]. However, the current knowledge mainly considers the effect of ammonia on PM formation. A recent study,[17] testing scenarios of agricultural emissions reductions, showed that in many densely populated areas, $PM_{2.5}$ aerosols formed from gases released by fertilizer application and animal husbandry can dominate over the combined contributions from all other anthropogenic pollution. The authors showed that the impact of livestock and fertilizers on

[1]UMR ECOSYS, INRAE, AgroParisTech, Université Paris-Saclay, 78850 Thiverval-Grignon, France. [2]Univ. Lille, CNRS, UMR 8523 - PhLAM - Physique des Lasers, Atomes et Molécules, F-59000 Lille, France. [3]Univ. Lille, CNRS, UMR 8522 - PC2A - Physicochimie des Processus de Combustion et de l'Atmosphère, F-59000 Lille, France. ✉email: raluca.ciuraru@inrae.fr

air quality is very pronounced in Europe, where agricultural $PM_{2.5}$ is responsible for 55% of the air pollution linked to human activities[17].

The recycling of different types of organic waste products (OWPs) from livestock, urban or industrial sources is currently being promoted as a substitute for mineral fertilizers for agricultural land[18]. The recycling of OWPs also represents an alternative to waste management via landfilling or incineration. OWP recycling in agriculture can increase the organic matter stocks in soil[19] and thereby improve soil chemical fertility, stimulate microbial activity, or increase water retention[20]. It also improves the recycling of nutrients and can decrease the use of mineral fertilizers[21], which are nonrenewable resources. However, the application of OWPs to agricultural soils can pose different health and environmental risks: some contaminants can accumulate in the soil, degrade water quality, or be emitted into the atmosphere[22]. In a peri-urban context, where the number of municipal wastewater treatment plants is continuously increasing through urbanization, sewage sludge production increased by 50% in European countries from 1992 to 2005, and a further increase in total sludge production is expected in the upcoming years[23]. In terms of final sludge disposal, 53% of the sludge produced is used in agricultural applications and composting[24].

Despite the continuously increasing number of new atmospheric particle formation measurements, we still lack regional observations of NPF processes. In agricultural areas, we have a limited understanding of the biosphere–atmosphere exchange of agriculturally emitted trace gases other than NH_3, and their contribution to secondary aerosols is missing[13]. The importance of the effect of agriculture on atmospheric NPF is expected to vary regionally, as well as over the course of the year.

Some studies have shown VOC emissions from organic fertilizers by laboratory measurements or small wind tunnel experiments[25–27]. To our knowledge, no work has addressed their contribution to SOAs to date. For instance, there are few studies dealing with VOC measurements from livestock fertilizers[27,28] or urban waste products[29,30], although such data are essential for a better understanding of the formation and fate of SOAs from agricultural practices. Research on VOC emissions is very challenging owing to the large number of VOCs and their variable physicochemical properties[31]. Our understanding of the chemistry of these VOCs is very limited compared with that of other agricultural pollutants, such as NH_3 or, more recently, hydrogen sulfide[32,33]. However, a certain number of VOCs observed in organic waste are now established SOA precursors, such as sulfur compounds (e.g., dimethyl and diethyl sulfide)[28,34]; terpenes (alpha-pinene, limonene)[30]; nitrogen-containing compounds, ketones, and aldehydes[35]; and aromatic compounds[29,31,36].

Simulations and atmospheric observations have shown that almost all nucleation processes involve ammonia or biogenic organic compounds in addition to sulfuric acid[3]. To date, agricultural secondary aerosol formation is thought to be mainly induced by nucleation of ammonia emissions[14]. Here, we report atmospheric particle formation solely from oxidized organic molecules and SO_2, which are both emitted by sewage sludge. The focus of this work is to identify the molecules that form new particles from sewage sludge and to understand the mechanism underlying particle formation and initial growth. To the best of our knowledge, this is the first time these aerosol formation phenomena have been observed and quantified in an agricultural system.

RESULTS AND DISCUSSION

Evidence of NPF from sewage sludge

Sewage sludge samples from a sewage treatment plant were introduced into a Teflon-coated reaction chamber and exposed to ambient levels of ozone (Supplementary Fig. 1). Prior to each ozonolysis experiment, the chamber was carefully cleaned, and extremely low contaminant concentrations were established (Supplementary Fig. 2).

Upon sample introduction into the chamber, a strong burst release of methylindole (m/z 132.087 $C_9H_9NH^+$) was observed. Following the initial burst, sewage VOC signals stabilized. Production of NH_3 and SO_2 was also observed. NO_x mixing ratios were low (2–3 ppb) during the experiments. Within a few seconds of the initial exposure of sewage sludge samples to O_3 in the chamber, the signal of m/z 132.087 $C_9H_9NH^+$ decreased, and those of gas-phase oxygenated and nitrogen-containing molecules, in particular m/z 136.075 $C_8H_9NOH^+$ and m/z 164.070 $C_9H_9NO_2H^+$, increased (Fig. 1c). The ozone mixing ratio was continuously monitored in the chamber and remained at ~55 ppbv at the entrance of the chamber during each experiment. Particles appeared almost instantaneously after O_3 injection. The particle number and size distributions (Fig. 1a) spanned the entire measured size range from 2 to 64 nm in electrical mobility diameter, indicating newly formed particles. During these experiments, the particle number concentration reached a maximum of 10^6 particles cm^{-3} within <2 min. This led to a particle nucleation rate up to $1.1 \times 10^6\ cm^{-3}\ s^{-1}$ during the NPF. At longer reaction times, the particles grew in size, and their number remained constant thereafter or slightly decreased, probably owing to coagulation and/or losses by adsorption to the walls. This behavior of the particle number concentration and size distribution was observed to be constant for experiments lasting as long as 5 hours.

Interestingly, ozone was not completely consumed during the experiment, which means that only ~20 ppb O_3 was needed for ozonolysis to form particles. Additional experiments performed under high excess ozone (250 ppb) did not show any difference in particle number or size distribution. This may indicate that the reaction is limited by the residence time (5 min) inside the chamber. A fast but not complete consumption of m/z 132.087 $C_9H_9NH^+$ was also observed, and the abundance of reaction products reached a plateau in <15 min. This may be due to the high kinetic rate constant for the reaction of m/z 132.087 $C_9H_9NH^+$ with ozone but might also indicate that oxidation can occur in both the gaseous and condensed phases (walls, sewage sludge surface or secondary aerosols).

Identification of key players in NPF

The VOC data measured with three independent techniques (proton transfer reaction mass spectrometry, PTR-ToF-MS; gas chromatography coupled to mass spectrometry, GC-MS; and ultra-high-performance liquid chromatography coupled to high-resolution mass spectrometry, UHPLC-HRMS) were compared to identify the detected ions. The identification was based on the retention time and mass spectrum of each compound. $C_9H_9NH^+$ (m/z 132.08) was identified as skatole. Skatole has been reported as one of the major malodorous compounds contributing to the odor problem of animal production facilities and sewage treatment plants and is emitted by bacterial degradation in a slurry[32,37]. Indoles belong to an important class of atmospheric VOCs with high atmospheric emissions from land spreading of OWPs and contribute to odor nuisance[27,38].

It was reported that indoles and skatole are very reactive nucleophiles and easily undergo electrophilic substitution reactions[39]. Only one study has reported the reaction rate constant in the aqueous phase for skatole with ozone at pH = 6.7 is $4.5 \times 10^6\ M^{-1}\ s^{-1}$ [40]. The authors reported a stoichiometric factor of 0.9, meaning that 1 mol of ozone is needed for ozonation of 0.9 mol of skatole[40], and the reaction rate constants of indolic compounds in water increase with pH. A rough estimation of the rate constant was performed based on skatole experiments, leading to a value

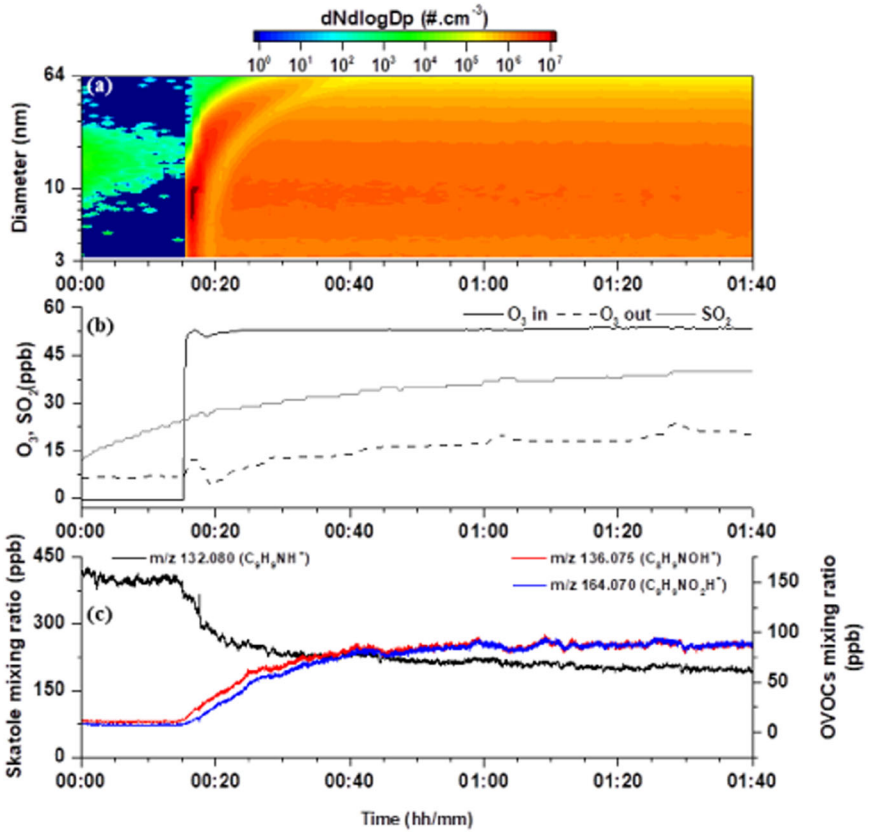

Fig. 1 Typical sewage sludge ozonolysis experiment. a Temporal evolution of the particle number concentration and size distribution. The ordinate represents the electrical mobility diameter (nm), and the color scale represents the particle number concentration. **b** Temporal evolution of O_3 entering the chamber (black line, O_3 in), O_3 measured at the exit of the chamber (black dotted line, O_3 out) and SO_2 (gray line). **c** Temporal evolution of m/z 132.080 $C_9H_9NH^+$ (black line, left axis), m/z 136.075 $C_8H_9NOH^+$ (red line, right axis), and m/z 164.070 $C_9H_9NO_2H^+$ (blue line, right axis).

of 5×10^{-15} cm^3 mol^{-1} s^{-1}. Such a rate constant would confirm that skatole is a very reactive compound towards ozone, resulting in a lifetime of ~3 min at typical ambient ozone concentrations. This is a higher reactivity than what was reported for indole (5×10^{-17} cm^3 mol^{-1} s^{-1})[41] or for the well-known alpha-pinene system (1×10^{-16} cm^3 mol^{-1} s^{-1})[42] but lower than that of some alkenes, such as alpha-terpinene or beta-caryophyllene (1×10^{-14} cm^3 mol^{-1} s^{-1})[43].

As shown in Fig. 1c, two oxygenated products were observed in the gas phase (m/z 136.075 $C_8H_9NOH^+$ and m/z 164.070 $C_9H_9NO_2H^+$) after the ozonolysis reactions. These oxidation products contain the carbon skeleton of their precursor skatole. Gas chromatography analysis performed before and after ozonolysis and liquid chromatography performed on collected particles revealed that m/z 164.070 $C_9H_9NO_2H^+$ corresponds to 2-acetyl phenyl formamide.

Multiple other VOCs were emitted by the sewage sludge samples. For example, acids (e.g., formic acid), alcohols (e.g., methanol, butanol), aldehydes, and ketones (acetone, butanone, acrolein), or sulfur-containing compounds (e.g., dimethyl sulfide, hydrogen sulfide) were measured, but most of these VOCs react very slowly with ozone. Isoprene and monoterpenes were also measured by PTR-TOF-MS in our experiments. However, all the ion signals were carefully verified, and the only decreasing ion that was observed, based on the PTR-TOF-MS measurements, was skatole. We cannot fully exclude the possibility that other VOCs might play a role in particle formation, but from our experiments, skatole is the only VOC evidenced as an aerosol precursor.

Proposed ozonolysis mechanism

The reaction of ozone with skatole proceeds via the Criegee mechanism, involving an initial O_3 addition to the double bound to yield a primary ozonide that decomposes into two stabilized Criegee intermediates (Fig. 2)[44]. As ozonolysis of skatole takes place at the endocyclic double bound, the carbonyl oxide and carbonyl moieties that should be formed are attached together as part of the same molecule[45,46]. The ozonolysis of endocyclic compounds may add several functional groups with no loss in carbon number, leading to the formation of secondary ozonides[47], which have been shown to make important contributions to SOAs[2].

The primary ozonide can enter two possible pathways: decomposition by cycle-based cleavage of the O-O bond distal from the methyl group (a) or cleavage of the O-O bond proximal to the methyl group (b). The first intermediate can undergo hydrogen shift reactions to form ketonic hydroperoxides or can isomerize to form dioxirane[44]. The second intermediate can form aldehydic hydroperoxides or cyclizes to form a secondary ozonide. Both can form a secondary ozonide via recyclization[44,45] (Fig. 2). Further decomposition of the O−OH bond in the hydroperoxides, which are thermally unstable[48], will lead to organic and OH radical formation[49]. On the other hand, Criegee intermediate 1 can react with a carbonyl and form the secondary ozonide $C_9H_9NO_3$ (m/z 179.057)[44]. The first intermediate can oxidize SO_2 and form the 2-acetyl phenyl formamide $C_9H_9NO_2$ (m/z 163.063) and SO_3. Hydrolysis of SO_3 leads to the formation of H_2SO_4. Reactions of Criegee intermediates formed during ozonolysis of certain alkenes with SO_2 can be significantly fast[50]. Moreover, this reaction is

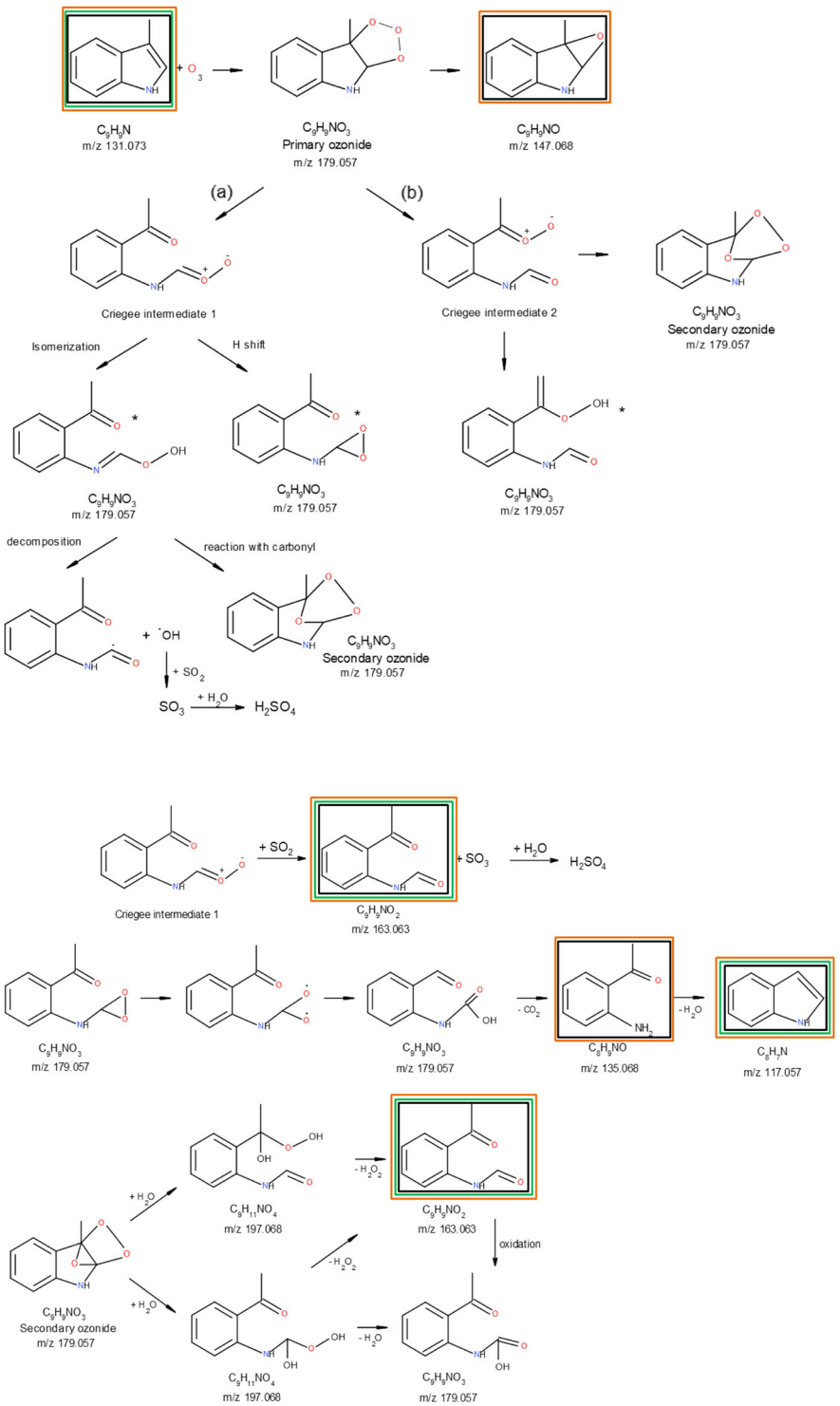

Fig. 2 Proposed mechanism of skatole ozonolysis. The compounds detected by PTR-ToF-MS are framed in black, those detected by GC-MS in green, and those detected by UHPLC-HRMS in orange.

characterized by 97% collisional stabilization and a low percentage of ring opening and SO_3 formation[51]. The secondary ozonide ($C_9H_9NO_3$) can react with water to form a molecule possessing an aldehyde or a ketone group and a hydroxy-hydroperoxide group (Fig. 2). The latter compound can lose H_2O_2 and form 2-acetyl phenyl formamide. Further oxidation of this compound leads to oxocarboxylic acid, which has been evidenced on the aerosol surface by two-step laser mass spectrometry (L2MS). Another possibility is that the hydroxy-hydroperoxide group loses water, and thus, 2-acetyl phenyl formamide is directly formed. Skatole oxide (m/z 148.075 $C_9H_9NOH^+$) was also observed in the gas phase from the ozonolysis reaction. It is now known that oxidation of SO_2 by stabilized Criegee intermediates represents a significant source of atmospheric sulfuric acid produced via SO_3 formation. SO_3 reacts very rapidly with water vapor to form H_2SO_4[50], which is a key atmospheric nucleation species[46]. The production of OH

radicals during ozonolysis of indoles will drive further chemistry, including oxidation of SO_2 to H_2SO_4[50]. Various field measurements and modeling studies have shown that stabilized Criegee intermediates could make a significant contribution (from 10 to 70%) to SO_2 oxidation[45]. Oxidation of SO_2 by a stabilized Criegee intermediate is a significant source of atmospheric sulfuric acid produced in VOC-rich environments[46]. The SO_2 emitted by sewage sludge will then react with Criegee intermediates to produce sulfuric acid. Moreover, SO_2 can also partition into aerosols to form HSO_3^-, which can further react with organic peroxides generated by skatole ozonolysis. This mechanism is consistent with literature data[52] and with the presence of this species on our collected particles. Secondary ion mass spectrometry (SIMS) surface analysis performed (negative ion polarity) on the newly formed particles collected on quartz filters during ozonolysis reactions revealed the presence of characteristic H_2SO_4 peaks such as SO_3^- and HSO_4^- peaks (Supplementary Fig. 4). Notably, SO_3^- and HSO_4^- ions were also detected in the sewage sludge bulk samples by SIMS (Supplementary Fig. 5). No sulfur-containing organic compounds were detected in the present study, but the possibility that organosulfates may have fragmented in the SIMS, contributing to the observed SO_3^- signal, cannot be excluded.

Another important pathway is the reaction of stabilized Criegee intermediates with water, leading to the formation of α-hydroxy hydroperoxides, organic acids, ketones and aldehydes, SO_2, NOx, and H_2O_2[45]. These reactions may also represent a significant source of OH and HOx radicals[44]. The observed products can therefore arise from the reaction of both ozone and OH radicals with these compounds.

Chemical composition of the aerosols

The chemical composition of the generated aerosols was studied using L2MS, SIMS, and UHPLC-HRMS. A high number of oxidized and bifunctional species was detected on the filter-sampled particles. Overall, L2MS revealed the formation of oxidized compounds not detected in the gas phase by PTR-ToF-MS or GC-MS. The observed compounds can be classified into different groups: a first group containing the carbon skeleton of skatole with inserted oxygen atoms (e.g., C_9H_9NO, $C_9H_9NO_2$, $C_9H_9NO_3$), a second group resulting from ring opening owing to successive oxidation processes (e.g., $C_9H_{17}NO$, $C_{11}H_{22}NO_2$), a third class with oxygen attached to the six-member ring (e.g., $C_8H_{13}NO_2$) and a fourth group with nitrogenated compounds (e.g., $C_9H_9N_2$, $C_{11}H_{20}N_2$, $C_{14}H_{21}N_2$) (Supplementary Fig. 6). Owing to the presence of multiple double bonds in skatole, multiple ozonolysis reactions are possible and consistent with the observation that SOAs continue to grow. All these reaction products might continue to evolve chemically, leading to a decrease in volatility and rapid partitioning to the particulate phase. 2-Acetyl phenyl formamide ($C_9H_9NO_2$) was also detected in the particulate phase by L2MS and UHPLC-HRMS and accounted for a large fraction of the identified products in the gas phase.

Furthermore, experiments performed on non-SO_2-emitting sewage samples showed no particle formation following skatole ozonolysis (Fig. 3). In light of these results, we propose a binary reaction mechanism involving organics and SO_2 via sulfuric acid formation.

Several studies performed on sewage sludge samples or sewage sludge compost showed the presence of different inorganic and sulfur organic compounds (hydrogen sulfide,

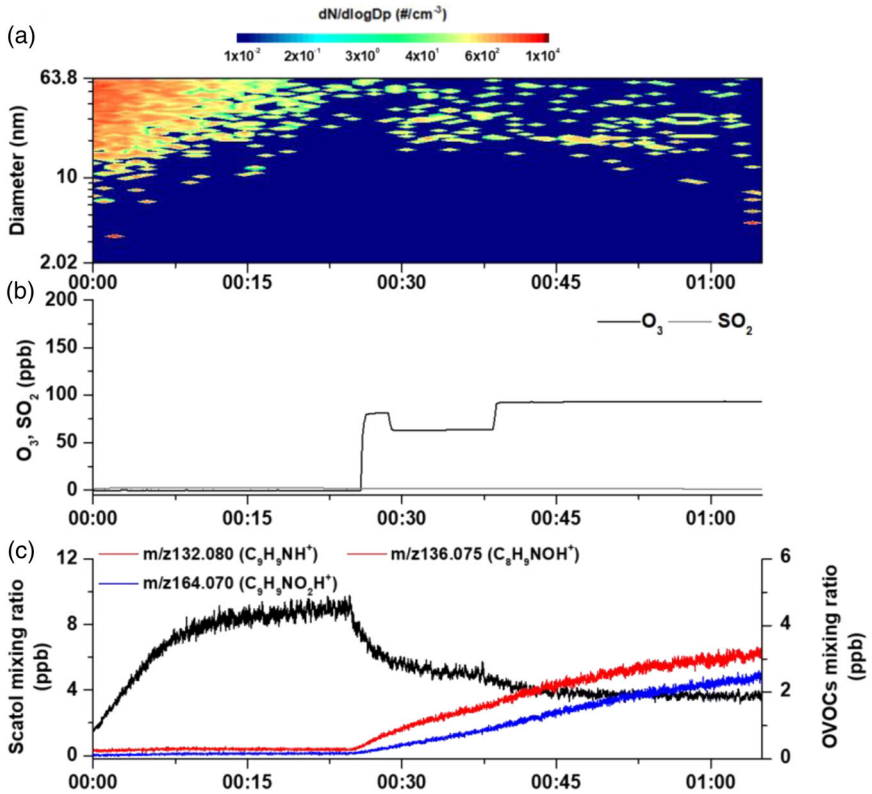

Fig. 3 Non-emitting SO_2 sewage sludge ozonolysis experiment. a Temporal evolution of the particle number concentration and size distribution. The ordinate represents the electrical mobility diameter (nm), and the color scale represents the particle number concentration. **b** Temporal evolution of O_3 entering the chamber (black line, O_3 in) and SO_2 (gray line). **c** Temporal evolution of m/z 132.080 $C_9H_9NH^+$ (black line, left axis), m/z 136.075 $C_8H_9NOH^+$ (red line, right axis), and m/z 164.070 $C_9H_9NO_2H^+$ (blue line, right axis).

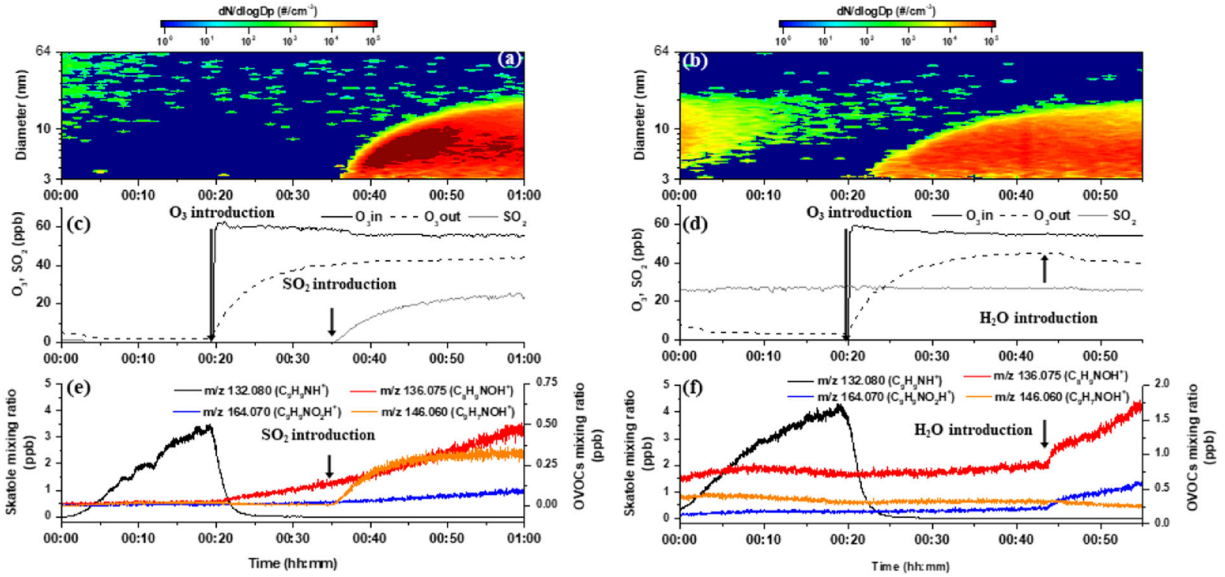

Fig. 4 Skatole ozonolysis experiment. a, **b** Temporal evolution of the particle number concentration and size distribution. **c**, **d** Temporal evolution of O_3 entering the chamber (black line), O_3 measured at the exit of the chamber (black dotted line) and SO_2 (gray line). **e**, **f** Temporal evolution of m/z 132.080 $C_9H_9NH^+$ (black line, left axis), m/z 136.075 $C_8H_9NOH^+$ (red line, right axis), m/z 146.060 $C_9H_7NOH^+$ (orange line, right axis), and m/z 164.070 $C_9H_9NO_2H^+$ (blue line, right axis). Left column: SO_2 introduction at 00:35 min; right column: H_2O introduction at 00:43 min.

methyl mercaptan, dimethyl sulfide, dimethyl disulfide, carbon disulfide) produced by anaerobic microorganisms. Sulfur-containing compounds are also produced by bacteria through the reduction of sulfate- and S-containing amino acids[53,54]. These amino acids are monomers of protein extracted from activated sludge and anaerobically digested sludge. Organic sulfur compounds from dewatered biosolids can be generated by the degradation of sulfur-containing amino acids and the methylation of sulfide and methanethiol. Furthermore, thermal treatment of sewage sludge leads to the emission of pollutants in the form of sulfur dioxide (SO_2)[54], and sewage sludge can contain high concentrations of sulfur compounds, resulting in high emissions of SO_2[34]. H_2S reacts rapidly with OH radicals with a rate constant of 4.7×10^{-12} cm^3 $molecule^{-1}$ s^{-1} and forms SO_2. It is possible then that SO_2 was formed by these reactions in our system. On the other hand, the reaction of H_2S with ozone was too slow to form SO_2 in our experiments[55].

Testing the skatole NPF hypothesis

To verify this hypothesis, we designed an experiment in which skatole reactivity was measured in an empty chamber. The goal was to test the effect of O_3, SO_2, and NH_3 on commercially available skatole. A pure skatole sample was introduced into the chamber, and as shown in Fig. 4, the skatole signal dropped dramatically after O_3 introduction, accompanied by a slow increase in m/z 136.075 $C_8H_9NOH^+$ and m/z 164.07 $C_9H_9NO_2H^+$. The reaction of ozone with skatole proceeds by initial O_3 addition to the double bound to yield a primary ozonide. However, no particle formation was observed following ozonolysis; therefore, we can discard the purely biogenic nucleation mechanism. Most likely, the volatility of skatole oxidation products is not low enough. Upon SO_2 introduction into the chamber, the formation of m/z 146.060 $C_9H_7NOH^+$ was observed, which may represent the product of the hydroperoxide pathway of the Criegee intermediate (Fig. 2). $C_8H_7NOH^+$ (m/z 136.060), corresponding to the ester pathway of the Criegee intermediate, was also observed in the gas phase after SO_2 introduction. The contribution of SO_2 to NPF is further illustrated in Fig. 4, which shows the prompt NPF event only when SO_2 is introduced into the chamber. This is consistent with sulfuric acid formation by reactions of SO_2 with stabilized Criegee intermediates[46]. Most likely, oxidation products of skatole are able to stabilize sulfuric acid clusters, enhancing the NPF observed. Skatole itself is a basic compound with a proton affinity similar to that of dimethyl amine (DMA), which has been found to be a key player in atmospheric nucleation[6]. From a molecular point of view, the key to the stabilization of molecular clusters of bases with sulfuric acid is proton transfer[56], as in the case of ammonia and sulfuric acid clusters. Classical nucleation theory (CNT) involves bulk properties, so it predicts proton transfer from the very first cluster containing one sulfuric acid molecule and one ammonia molecule. However, quantum mechanics (QM)-based chemical calculations have shown that this is not the case, as one will need at least two molecules for the proton to be transferred. When converted into evaporation rates of clusters calculated by CNT and QM, there are differences of several orders of magnitude. In the case of DMA, proton transfer occurs from the very beginning, with just one molecule of sulfuric acid; this explains why DMA can enhance the nucleation of sulfuric acid much more than ammonia[8,56] and is why we compared DMA with skatole in terms of proton affinity. Another important molecular feature for a base to be able to enhance nucleation effectively seems to be having an additional H atom attached to the N atom so it can form hydrogen bonds with more than one sulfuric acid molecule[56]. As in DMA, skatole contains a hydrogen atom attached to the N atom, so we believe that this might also enable skatole to enhance sulfuric acid nucleation, as does DMA. Dedicated quantum chemical calculations, which are out of the scope of this paper, might be relevant in this case and could confirm our hypothesis.

Other basic compounds, such as indoles, are produced during skatole oxidation. Furthermore, all oxidation products of skatole retain the N atom in their structure, even if they also possess a carboxylic acid group. From a molecular point of view, having both an NH group and a carboxylic acid group can facilitate the formation of clusters with several molecules of sulfuric acid. Indeed, the theoretical simulations performed by Elm et al.[57] show how small amino acids can effectively stabilize sulfuric acid clusters, thus playing an important role in atmospheric NPF. The aerosol number concentration reaches its maximum when SO_2 is introduced. It is also interesting to observe the different particle

sizes: smaller particles are formed in skatole-controlled experiments than in sewage sludge experiments, revealing the potential role of other VOCs that might contribute to particle growth. In a second step, ozone was introduced into the chamber while skatole and SO_2 mixing ratios were kept constant. Likewise, the skatole signal decreased shortly after O_3 was added (Fig. 4f), accompanied by a concurrent NPF event (Fig. 4b), confirming the need for sulfuric acid and oxidation products of skatole to produce new particles.

In a third step, water vapor was added into the chamber (from dry conditions to 90% RH). As shown in Fig. 4f, water introduction led to an increase in the m/z 136.075 $C_8H_9NOH^+$ and m/z 164.07 $C_9H_9NO_2H^+$ signals in the gas phase. The signal for stabilized Criegee m/z 146.060 $C_9H_7NOH^+$ slightly decreased. This species might react with water vapor to form a carbonyl compound and H_2O_2. The increase in m/z 164.070 in the presence of water indicates possible competition between the water vapor and the Criegee intermediates. In the first set of experiments when the RH was very low (Fig. 4e), m/z 146.060 $C_9H_7NOH^+$ formed when SO_2 was introduced, whereas at high RH, the formation of 2-acetyl phenyl formamide was detected. In contrast, water vapor had no effect on the aerosol particle number concentration.

The same types of experiments were performed to test the effect of NH_3 on NPF. As in the case of SO_2, NH_3 was injected into the chamber during skatole ozonolysis. No NPF was observed during the NH_3 injection (Supplementary Fig. S3). Seeing these results, we can conclude that most likely the NPF mechanism behind the observed nucleation events consists of sulfuric acid nucleation enhanced by the oxidation products of skatole acting as bases, as in the case of ammonia or amine nucleation reported in the literature[5,6].

Atmospheric implications

This study provides insights into gaseous emissions and aerosol formation from OWPs and clearly points towards an impact of processes at the air-soil interface.

Agriculture contributes ~16% of $PM_{2.5}$ primary emissions and ~18% of PM_{10} emissions[13]. However, there is no estimate of SOA formation from precursor gases emitted from the agricultural sector[14]. Recent studies have shown that aerosol formation in regions with intensive ammonia emissions may have been underestimated. A large part of the gap between modeled and measured aerosol concentrations might be explained by these underestimated agricultural sources[14]. Moreover, agricultural particles are thought to be generated during specific operations and processes or formed as secondary particles from NH_3 emissions. In this study, an NPF mechanism involving agricultural materials that does not involve ammonia is highlighted.

This study shows that indoles, and more specifically skatole, together with SO_2 emitted by sewage sludge, are the species pertinent to initiating reactions with atmospherically relevant ozone mixing ratios, leading to particle nucleation and growth events. Indole compounds are present at the field scale during spreading on agricultural surfaces. For example, production and release of 4.91–8.3 μg m^{-2} min^{-1} skatole following land spreading of pig slurry[27] or land application of swine manure slurry[58] have been shown in the literature. Skatole emissions of ~50 μg m^{-2} min^{-1} were estimated in the present work (details in the Supplementary Information). Various reaction products were observed in the gaseous and particulate phases. Among them, 2-acetyl phenyl formamide was identified as the main skatole ozonolysis product, and formation pathways were proposed. Furthermore, chemical analysis of particles showed that organic compounds contribute to growth in this size range. All these statements are supported by chamber measurements using commercially available skatole. The high reactivity of skatole towards ozone results in considerable enhancement of condensable reaction products that might partition into the aerosol phase and potentially act as cloud condensation nuclei[3].

The particle mass (2.9 μg m^{-3}) and number (5×10^6 # cm^{-3}) concentrations measured in our experiments exceed some of the field measurements conducted at various locations and the measurements in other laboratory experiments performed on agricultural samples. Our study revealed a particle nucleation rate up to 1.1 10^6 cm^{-3} s^{-1} during NPF. For example, the laboratory study of Joutsensaari et al.[59] found an aerosol number concentration of 5.5×10^3 # cm^{-3} from the ozonolysis of VOCs emitted by living white cabbage plants and a particle formation rate of ~3 cm^{-3} s^{-1} (over a particle diameter range of 5.5–70 nm). Our numbers are higher than the particle formation rates observed in the atmosphere, which are often in the range of 0.01–10 cm^{-3} s^{-1} in the boundary layer (for 3 nm particles). However, it has been shown that in urban, coastal areas and industrial plumes, the formation rates are higher, up to 100 cm^{-3} s^{-1} and 10^4–10^5 cm^{-3} s^{-1}, respectively[12]. In our experiments, emissions were constrained by the volume of the chamber. In the real atmosphere, they would certainly be more diluted, leading to a lower concentration of precursors. However, in the chamber, the reaction time was limited to the residence time (5 min). In the atmosphere, the ozonolysis of skatole will not be limited to 5 min; thus, oxidation will occur all along the emission plume. It is obvious that longer oxidation will lead to more oxidized compounds that will contribute to particle formation. Finally, despite the difficult comparison of our results with real atmospheric processes, this work evidence the very large potential of sludge emissions as a strong contributor to particle formation.

Based on the particle emission flux in our experiments, on the surface area of sewage sludge spread in France and on the time before sewage sludge incorporation into the soil (48 h, according to French legislation), our results indicate a contribution of 0.94 tons of particles per year. This value represents 0.03% of total $PM_{1.0}$ emissions from the agriculture and forestry sectors in France based on annual national emissions inventories (details in the Supplementary Information). Given that spreading of sewage sludge takes place only a few days per year, usually in the middle of the summer, the contribution in mid-summer will not be negligible compared with that of other PM emission sources. The emissions from agricultural activities may be of concern for local and regional air quality during the time after spreading. The numbers would be higher if the particle number instead of the particle mass is considered. Indeed, high nucleation rates were observed, but the newly formed particles had a very low diameter and, as a result, a low mass. NPF from OWP spreading contributes significantly to atmospheric aerosol particle number concentrations, which might be a significant source of cloud condensation nuclei and alter cloud albedo, structure and lifetime.

The experiments carried out in this work, designed to match atmospheric conditions as closely as possible, might be applicable to NPF and growth in the atmosphere, as the ozone concentrations used in our study approached tropospheric levels, even at remote locations during spring and summer. SOA yields were calculated from the ratio of the formed SOA amount to the amount of skatole reacted, considering a density of aerosol particles of 1.0 g cm^{-3}. The SOA yields varied significantly among the experiments, with an average of 2.45%. Values for the SOA yield of skatole ozonolysis are not available in the literature. However, ozonolysis of biogenic terpenes has been characterized in simulation chambers, revealing SOA yields that varied over a broad range: mass yields of 0.16 and 0.21 for α-pinene ozonolysis were found[60], whereas some other studies reported SOA yields between 0 and 76% for the ozonolysis of monoterpenes[61]. Donahue et al.[62] explained the critical factors for SOA formation from terpene ozonolysis. The authors showed that different competing factors could affect the yield: oxygenation, which increases the absolute yield because the compounds are more

polar and thus less volatile, and the potential difference between gas phase and condensed phase oxidation and oligomerization. The same authors suggested that SOA yields are likely to increase substantially through several generations of oxidative processing of the semivolatile products. It has also been shown that SOA yields are 80–100% larger for loadings above 2 μg m^{-3}. Our SOA yields were lower than the yields of some monoterpenes, which might be explained by the aerosol mass loadings of ~3 μg m^{-3} and by the presence of oxygenated compounds and possible heterogeneous reactions at the sewage surface not taken into account in the yield calculations. A longer reaction time from experiments conducted in a larger facility would also lead to more oxidation and thus increase the transfer from the gas to the particle phase. Our findings imply that during sewage sludge spreading, skatole is an important potential contributor to the formation of new particles under atmospherically relevant conditions. As the application of OWPs is expected to increase with continuously growing agricultural activities[13], this additional VOC source may have a significant influence on atmospheric NPF and ozone reactivity during the spreading period. This study presents a mechanism involving indoles of agricultural origin. Even though we cannot apply these values directly to the atmosphere, our results suggest that these skatole emissions can change the chemistry and oxidative capacity of the atmosphere via their contribution to local concentrations. Even if they are not realistic under atmospheric conditions, these processes can make a qualitative contribution to particle numbers, as a high nucleation rate can locally and briefly induce the formation of a significant annual source of particles.

METHODS

Simulation chamber

The experiments were performed in a poly(methyl methacrylate) chamber with Teflon walls (0.03 m^3, 0.2 m height, 0.27 m width, 0.55 m length) built in a temperature-controlled room. A stainless steel container (0.52 × 0.27 × 0.02 m^3) filled with a sewage sludge sample was used. High-purity dry air (Air Liquide), passed through two Restek super clean gas filter kits for oxygen, moisture, and hydrocarbon removal (Restek, 22020) and an additional hydrocarbon trap (Restek 21991), was used for the experiments. The residence time of the air in the chamber was 5 min. The temperature and relative humidity in the chamber were 293 K and 40%, respectively. Before each experiment, the chamber was flushed with purified dry air for 30 min with a flow rate of 10 L min^{-1} until the particle number concentration in the chamber was below 1 particle cm^{-3}. When the VOC concentration reached an approximate steady state, ozone was injected, reaching a chamber concentration of approximately 55 ppb. No OH or Criegee intermediate scavengers were added, and no seed aerosol was used. Fifteen experiments with authentic sewage sludge samples (Supplementary Table 1) and two experiments with commercially available skatole (Sigma Aldrich >98.0% purity) were performed. Sewage sludge was sampled from the Colmar France sewage treatment plant.

Gas-phase analysis

The gas and particle phases were continuously sampled. A high-resolution proton transfer reaction time-of-flight mass spectrometer[36] (HR-Qi-PTR-ToF-MS, Ionicon Analytik GmbH) was used to measure the gas-phase VOC concentration in real time (temporal resolution of 1 s, m/z range of 10–510). The drift tube pressure was set to 4 mbar, the temperature to 80 °C, and the drift voltage to 1000 V. The extraction voltage at the end of the tube (UDx) was 44 V. The E/N was 132 Td (1 Td = 10^{-17} V cm^2). Protonated water ($H_3{}^{18}O^+$, m/z 21.022), protonated acetone ($C_3H_7O^+$, m/z 59.049) and protonated diiodobenzene (PerMaSCal Ionicon, $C_6H_5I_2^+$) ions and fragments ($C_6H_4I_2H^+$, m/z 330.941, and $C_6H_5I^+$, m/z 203.943, respectively) were used for mass calibration. All data obtained by PTR-ToF-MS were analyzed with PTR-MS Viewer software (version 3.1.1, IONICON Analytik). O_3 was introduced into the chamber via an ozone generator (OSG-1, UVP) using purified dry air as the carrier gas. The ozone at the entrance and at the exit of the chamber (41M, Environment SA), NO_x (model 42i-TL, Thermo Fisher Scientific, Inc.), SO_2 (model 43C, Thermo Environmental Instruments), NH_3 (Picarro G2103), CO_2 and H_2O (LICOR LI-840A) were continuously measured. VOCs were also trapped on Tenax TA cartridges for thermal desorption—gas chromatography—mass spectrometry analysis. The gas phase was sampled for 1 to 2 h at 0.4 L min^{-1} and regulated with a mass flow controller (Bronkhorst). Tubes were desorbed using a thermodesorption unit (Gerstel). VOC separation was carried out using an Agilent 7890B gas chromatograph on a capillary column (30 m length, 0.25 mm inner diameter, 0.25 μm film thickness, HP-5 MS Ultra Inert, Agilent). VOC detection was performed with an Agilent 5977A mass selective detector. Ozone, NO_x and SO_2 analyzers were calibrated before the experiments by the French air quality survey network. The PTR-ToF-MS was calibrated using a standard of 102 ± 10 ppb gaseous toluene in a bottle.

Particle analysis

The particle number concentration and size distribution were measured using a scanning mobility particle sizer (SMPS 3938; TSI) consisting of a DMA (TSI 3085) and a condensation particle counter (TSI 3788), which are extensively described elsewhere[63]. Sample flow was fixed at 0.6 L min^{-1} and sheath flow at 6 L min^{-1}, providing measurements of the particle number and size distribution between 2.64 and 64 nm in electrical mobility diameter. In the present study, it was assumed that the wall loss rate was constant during the experiments. All the values were wall and tube loss corrected (a maximum of 5% wall loss correction was applied to smaller diameters) based on Kulkarni et al.[64]. The particle number and size distribution measured with the SMPS were used to estimate the nucleation rates following the methodology described by Kulmala et al.[65]. The freshly formed secondary aerosols were collected for 3–5 h on quartz fiber filters (Pall Tissuquartz QAT-UP 2500, 14 mm diameter) before chemical characterization by mass spectrometry techniques and liquid chromatography. The surface chemical composition of pristine sewage sludge before ozonolysis was also analyzed by time-of-flight secondary ion mass spectrometry (TOF-SIMS). The TOF-SIMS analyses of bulk sewage sludge and filter-sampled particles were performed with an IONTOF TOF.$SIMS_5$ instrument equipped with a Bi_3^+ primary ion source. The energy of the Bi_3^+ ions was set to 25 keV, and the dose used was ~ $2\,10^{11}$ ions cm^{-2}, which matched the static mode in which only moderate fragmentation is expected[66]. Both positive and negative ion polarities were investigated with mass resolutions $m/\Delta m$ of 2000 and 3000, respectively.

L2MS measurements were performed using a Fasmatech S&T instrument described elsewhere[67] and with an average mass resolution of $m/\Delta m$ ~ 8000. Desorption and ionization were achieved using two nanosecond Nd:YAG (Quantel Brilliant) pulsed lasers operated at 532 nm and 266 nm wavelengths, respectively. Laser energies were adjusted to maximize the ion signal while limiting fragmentation of the parent species. A limit of detection as low as ~0.2 femtomoles per laser pulse has been demonstrated in this configuration[68].

For UHPLC-HRMS analyses, the filters were extracted with methanol. Two methylindole, five methylindole, and three methylindole (skatole) standards with >98.0% purity were obtained from Sigma Aldrich and used as analytical standards for UHPLC calibration. The UHPLC analyses were performed using an Acquity BEH C18 column (100 × 2.1 mm, 1.7 μm particle size, Waters). The mobile phase consisted of LC/MS-grade acetonitrile/H_2O/0.1% formic acid at a 0.3 mL min^{-1} flow rate (gradient elution). The column temperature was set to 30 °C, and 10 μL of sample was injected. High-resolution mass spectrometry analysis was carried out with a Q-Exactive Orbitrap mass spectrometer (Thermo Fisher Scientific) in positive mode with a heated electrospray ionization probe using a high-resolution full scan. The mass resolution was 70,000 over the full range, m/z 70–500.

DATA AVAILABILITY

The data that support the findings of this study are available from the authors on reasonable request, see author contributions for specific data sets.

Received: 30 July 2020; Accepted: 23 December 2020;
Published online: 28 January 2021

REFERENCES

1. Burnett, R. et al. Global estimates of mortality associated with long-term exposure to outdoor fine particulate matter. *Proc. Natl Acad. Sci.* **115**, 9592–9597 (2018).

2. Kroll, J. H. & Seinfeld, J. H. Chemistry of secondary organic aerosol: formation and evolution of low-volatility organics in the atmosphere. *Atmos. Environ.* **42**, 3593–3624 (2008).
3. Lee, S.-H. et al. New particle formation in the atmosphere: from molecular clusters to global climate. *J. Geophys. Res. Atmos.* **124**, 7098–7146 (2019).
4. Kulmala, M. et al. Direct observations of atmospheric aerosol nucleation. *Science* **339**, 943–946 (2013).
5. Kirkby, J. et al. Role of sulphuric acid, ammonia and galactic cosmic rays in atmospheric aerosol nucleation. *Nature* **476**, 429–433 (2011).
6. Almeida, J. et al. Molecular understanding of sulphuric acid–amine particle nucleation in the atmosphere. *Nature* **502**, 359–363 (2013).
7. Riccobono, F. et al. Oxidation products of biogenic emissions contribute to nucleation of atmospheric particles. *Science* **344**, 717–721 (2014).
8. Kirkby, J. et al. Ion-induced nucleation of pure biogenic particles. *Nature* **533**, 521–526 (2016).
9. Ehn, M. et al. A large source of low-volatility secondary organic aerosol. *Nature* **506**, 476–479 (2014).
10. Öström, E. et al. Modeling the role of highly oxidized multifunctional organic molecules for the growth of new particles over the boreal forest region. *Atmos. Chem. Phys.* **17**, 8887–8901 (2017).
11. Chrit, M. et al. Modelling organic aerosol concentrations and properties during ChArMEx summer campaigns of 2012 and 2013 in the western Mediterranean region. *Atmos. Chem. Phys.* **17**, 12509–12531 (2017).
12. Kulmala, M. et al. Formation and growth rates of ultrafine atmospheric particles: a review of observations. *J. Aerosol. Sci.* **35**, 143–176 (2004).
13. Aneja, V. P., Schlesinger, W. H. & Erisman, J. W. Effects of agriculture upon the air quality and climate: research, policy, and regulations. *Environ. Sci. Technol.* **43**, 4234–4240 (2009).
14. Lelieveld, J., Evans, J. S., Fnais, M., Giannadaki, D. & Pozzer, A. The contribution of outdoor air pollution sources to premature mortality on a global scale. *Nature* **525**, 367–371 (2015).
15. Vuolo, R. M. et al. Nitrogen oxides and ozone fluxes from an oilseed-rape management cycle: the influence of cattle slurry application. *Biogeosciences* **14**, 2225–2244 (2017).
16. Faburé, J. et al. Bibliography review of the agricultural contribution in atmospheric particles emissions: identification of emission factors. *INRA Paris*, pp 164 (2011).
17. Bauer, S. E., Tsigaridis, K. & Miller, R. Significant atmospheric aerosol pollution caused by world food cultivation. *Geophys. Res. Lett.* **43**, 5394–5400 (2016).
18. European Commission. Communication from the Commission to the Council and the European Parliament on future steps in bio-waste management in the European Union. https://eur-lex.europa.eu/legal-content/EN/TXT/?uri=celex:52010DC0235 (2010).
19. Peltre, C. et al. RothC simulation of carbon accumulation in soil after repeated application of widely different organic amendments. *Soil Biol. Biochem.* **52**, 49–60 (2012).
20. Diacono, M. & Montemurro, F. Long-term effects of organic amendments on soil fertility. A Review. *Agron. Sustain. Dev.* **30**, 401–422 (2010).
21. Gutser, R., Ebertseder, T. H., Weber, A., Schraml, M. & Schmidhalter, U. Short-term and residual availability of nitrogen after long-term application of organic fertilizers on arable land. *J. Plant Nutr. Soil Sci.* **168**, 439–446 (2005).
22. Houot, S. et al. *Agronomic Value and Environmental Impacts of Urban Composts Used in Agriculture*. in Microbiology of Composting (eds. Insam, U. D. D. H., Sc, N. R. M. & Klammer, M. S.) 457–472 (Springer Berlin Heidelberg, 2002).
23. Bianchini, A., Bonfiglioli, L., Pellegrini, M. & Saccani, C. Sewage sludge management in Europe: a critical analysis of data quality. *Int. J. Environ. Waste Manag.* **18**, 226 (2016).
24. Kelessidis, A. & Stasinakis, A. S. Comparative study of the methods used for treatment and final disposal of sewage sludge in European countries. *Waste Manag* **32**, 1186–1195 (2012).
25. Kumar, A. et al. Volatile organic compound emissions from green waste composting: characterization and ozone formation. *Atmos. Environ.* **45**, 1841–1848 (2011).
26. Potard, K. et al. Organic amendment practices as possible drivers of biogenic volatile organic compounds emitted by soils in agrosystems. *Agric. Ecosyst. Environ.* **250**, 25–36 (2017).
27. Liu, D., Nyord, T., Rong, L. & Feilberg, A. Real-time quantification of emissions of volatile organic compounds from land spreading of pig slurry measured by PTR-MS and wind tunnels. *Sci. Total Environ.* **639**, 1079–1087 (2018).
28. Feilberg, A., Bildsoe, P. & Nyord, T. Application of PTR-MS for measuring odorant emissions from soil application of manure slurry. *Sensors* **15**, 1148–1167 (2015).
29. Nie, E. et al. Emission characteristics of VOCs and potential ozone formation from a full-scale sewage sludge composting plant. *Sci. Total Environ.* **659**, 664–672 (2019).
30. Rincón, C. A. et al. Chemical and odor characterization of gas emissions released during composting of solid wastes and digestates. *J. Environ. Manag.* **233**, 39–53 (2019).
31. Harrison, E. Z., Oakes, S. R., Hysell, M. & Hay, A. Organic chemicals in sewage sludges. *Sci. Total Environ.* **367**, 481–497 (2006).
32. Ni, J.-Q., Robarge, W. P., Xiao, C. & Heber, A. J. Volatile organic compounds at swine facilities: a critical review. *Chemosphere* **89**, 769–788 (2012).
33. Feilberg, A., Hansen, M. J., Liu, D. & Nyord, T. Contribution of livestock H2S to total sulfur emissions in a region with intensive animal production. *Nat. Commun.* **8**, 1069 (2017).
34. Byliński, H., Barczak, R. J., Gębicki, J. & Namieśnik, J. Monitoring of odors emitted from stabilized dewatered sludge subjected to aging using proton transfer reaction-mass spectrometry. *Environ. Sci. Pollut. Res.* **26**, 5500–5513 (2019).
35. Sánchez-Monedero, M. A., Fernández-Hernández, A., Higashikawa, F. S. & Cayuela, M. L. Relationships between emitted volatile organic compounds and their concentration in the pile during municipal solid waste composting. *Waste Manag* **79**, 179–187 (2018).
36. Abis, L. et al. Profiles of volatile organic compound emissions from soils amended with organic waste products. *Sci. Total Environ.* **636**, 1333–1343 (2018).
37. Gebicki, J., Byliński, H. & Namieśnik, J. Measurement techniques for assessing the olfactory impact of municipal sewage treatment plants. *Environ. Monit. Assess.* **188**, 32 (2015).
38. Woodbury, B. L. et al. Emission of volatile organic compounds after land application of cattle manure. *J. Environ. Qual.* **43**, 1207 (2014).
39. Sundberg, R. J. The chemistry of indoles. (Academic Press, 1970).
40. Wu, J. J. & Masten, S. J. Oxidation kinetics of phenolic and indolic compounds by ozone: applications to synthetic and real swine manure slurry. *Water Res.* **36**, 1513–1526 (2002).
41. Atkinson, R., Tuazon, E. C., Arey, J. & Aschmann, S. M. Atmospheric and indoor chemistry of gas-phase indole, quinoline, and isoquinoline. *Atmos. Environ.* **29**, 3423–3432 (1995).
42. Duncianu, M. et al. Development of a new flow reactor for kinetic studies. Application to the ozonolysis of a series of alkenes. *J. Phys. Chem. A* **116**, 6169–6179 (2012).
43. Calvert, J. G., Orlando, J. J., Stockwell, W. R. & Wallington, T. J. The mechanisms of reactions influencing atmospheric ozone. (Oxford University Press, 2015).
44. Donahue, N. M., Drozd, G. T., Epstein, S. A., Presto, A. A. & Kroll, J. H. Adventures in ozoneland: down the rabbit-hole. *Phys. Chem. Chem. Phys.* **13**, 10848 (2011).
45. Khan, Ma. H., Percival, C. J., Caravan, R. L., Taatjes, C. A. & Shallcross, D. E. Criegee intermediates and their impacts on the troposphere. *Environ. Sci. Process. Impacts* **20**, 437–453 (2018).
46. Boy, M. et al. Oxidation of SO2 by stabilized Criegee intermediate (sCI) radicals as a crucial source for atmospheric sulfuric acid concentrations. *Atmos. Chem. Phys.* **13**, 3865–3879 (2013).
47. Chuong, B., Zhang, J. & Donahue, N. M. Cycloalkene ozonolysis: collisionally mediated mechanistic branching. *J. Am. Chem. Soc.* **126**, 12363–12373 (2004).
48. Kroll, J. H., Sahay, S. R., Anderson, J. G., Demerjian, K. L. & Donahue, N. M. Mechanism of HOx formation in the gas-phase ozone-alkene reaction. 2. prompt versus thermal dissociation of carbonyl oxides to form OH. *J. Phys. Chem. A* **105**, 4446–4457 (2001).
49. Kurtén, T. & Donahue, N. M. MRCISD studies of the dissociation of vinylhydroperoxide, CH2CHOOH: there is a saddle point. *J. Phys. Chem. A* **116**, 6823–6830 (2012).
50. Mauldin, R. L. III et al. A new atmospherically relevant oxidant of sulphur dioxide. *Nature* **488**, 193–196 (2012).
51. Vereecken, L., Harder, H. & Novelli, A. The reaction of Criegee intermediates with NO, RO2, and SO2, and their fate in the atmosphere. *Phys. Chem. Chem. Phys.* **14**, 14682 (2012).
52. Ye, J., Abbatt, J. P. D. & Chan, A. W. H. Novel pathway of SO2 oxidation in the atmosphere: reactions with monoterpene ozonolysis intermediates and secondary organic aerosol. *Atmos. Chem. Phys.* **18**, 5549–5565 (2018).
53. Higgins, M. J. et al. Cycling of volatile organic sulfur compounds in anaerobically digested biosolids and its implications for odors. *Water Environ. Res.* **78**, 243–252 (2006).
54. Zhu, Y. et al. Odor composition analysis and odor indicator selection during sewage sludge composting. *J. Air Waste Manag. Assoc.* **66**, 930–940 (2016).
55. Atkinson, R. et al. Evaluated kinetic and photochemical data for atmospheric chemistry: volume I - gas phase reactions of Ox, HOx, NOx and SOx species. *Atmos. Chem. Phys.* **4**, 1461–1738 (2004).
56. Kurtén, T., Loukonen, V., Vehkamäki, H. & Kulmala, M. Amines are likely to enhance neutral and ion-induced sulfuric acid-water nucleation in the atmosphere more effectively than ammonia. *Atmos. Chem. Phys.* **8**, 4095–4103 (2008).
57. Elm, J., Fard, M., Bilde, M. & Mikkelsen, K. V. Interaction of glycine with common atmospheric nucleation precursors. *J. Phys. Chem. A* **117**, 12990–12997 (2013).
58. Parker, D. B. et al. Odorous VOC emission following land application of swine manure slurry. *Atmos. Environ.* **66**, 91–100 (2013).
59. Joutsensaari, J. et al. Nanoparticle formation by ozonolysis of inducible plant volatiles. *Atmos. Chem. Phys.* **5**, 1489–1495 (2005).

60. Xavier, C. et al. Aerosol mass yields of selected biogenic volatile organic compounds - a theoretical study with nearly explicit gas-phase chemistry. *Atmos. Chem. Phys.* **19**, 13741–13758 (2019).
61. Lee, A. et al. Gas-phase products and secondary aerosol yields from the ozonolysis of ten different terpenes. *J. Geophys. Res.* **111**, D07302 (2006).
62. Donahue, N. M. et al. Critical factors determining the variation in SOA yields from terpene ozonolysis: a combined experimental and computational study. *Faraday Discuss* **130**, 295 (2005).
63. Kammer, J. et al. Observation of nighttime new particle formation over the French Landes forest. *Sci. Total Environ.* **621**, 1084–1092 (2018).
64. Kulkarni, P., Baron, P. A. & Willeke, K. *Aerosol Measurement: Principles, Techniques, and Applications*. (John Wiley & Sons, Inc., 2011).
65. Kulmala, M. et al. Measurement of the nucleation of atmospheric aerosol particles. *Nat. Protoc.* **7**, 1651–1667 (2012).
66. Irimiea, C. et al. A comprehensive protocol for chemical analysis of flame combustion emissions by secondary ion mass spectrometry. *Rapid Commun. Mass Spectrom.* **32**, 1015–1025 (2018).
67. Duca, D. et al. On the benefits of using multivariate analysis in mass spectrometric studies of combustion-generated aerosols. *Faraday Discuss* **218**, 115–137 (2019).
68. Faccinetto, A., Focsa, C., Desgroux, P. & Ziskind, M. Progress toward the quantitative analysis of PAHs adsorbed on soot by laser desorption/lser ionization/time-of-flight mass spectrometry. *Environ. Sci. Technol.* **49**, 10510–10520 (2015).

ACKNOWLEDGEMENTS

This work was supported by the French national programme LEFE/INSU (ENGRAIS) no. 1762C0001, INRA EA department programme "Pari Scientifique" and ADEME (RAVISA) no. 1662C0006. This work also benefited from the support of ANAEE-FR services 592 (ANR project no. 11-INBS-0001). This work was also supported by the French National Research Agency (ANR) under contract ANR-18-CE22-0019 (UNREAL) and through the PIA (Programme d'Investissement d'Avenir) under contract ANR-10-LABX-005 (LABEX CaPPA – Chemical and Physical Properties of the Atmosphere). The authors thank Brigitte Pollet and Pascale Lieben for UHPLC analysis and Denis Montenach and Magali Imhoff for the sewage sludge samples.

AUTHOR CONTRIBUTIONS

R.C. designed the study, performed chamber experiments and wrote the manuscript. J.K., C.B., F.La., and D.P. performed chamber experiments and/or analyzed the PTR-ToF-MS and SMPS data. C.D. performed GC-MS analysis and analyzed the data. M.V., K.H., Y.C., C.F. performed the L2MS and SIMS experiments and analyzed the resulting data. M.B-D. helped with the UHPLC-HRMS mass spectrometer data. F.Le. and S.H. provided expertize in organic waste recycling and contributed to the manuscript. B.L., D.P., and I.K.O. contributed to the manuscript. C.F. performed data interpretation and critical editing and review of the manuscript. All authors commented on the manuscript.

COMPETING INTERESTS

The authors declare no competing interests.

ADDITIONAL INFORMATION

The online version contains supplementary material available at https://doi.org/10.1038/s41612-021-00160-3.

Correspondence and requests for materials should be addressed to R.C.

Reprints and permission information is available at http://www.nature.com/reprints

Publisher's note Springer Nature remains neutral with regard to jurisdictional claims in published maps and institutional affiliations.